

# Effect of Solvent Nature in Casting-Based Carbon Nanofiber/Poly(methyl-methacrylate) Nanocomposites

Helena Varela-Rizo, Iluminada Rodriguez-Pastor, Ignacio Martin-Gullon

Chemical Engineering Department, University of Alicante, PO Box E-03080, Alicante, Spain

Received 29 July 2011; accepted 17 November 2011

DOI 10.1002/app.36511

Published online 1 February 2012 in Wiley Online Library (wileyonlinelibrary.com).

**ABSTRACT:** Eight different solvents, of different polarities, were used to prepare carbon nanofiber (CNF)/poly(methyl methacrylate) nanocomposites by solvent casting. Selected solvents ranged from organic acetone to nonpolar toluene, passing through *N*-containing solvents. In addition, pristine and oxygen and nitrogen-functionalized CNFs were used. Two objectives were pursued: (1) the role of the solvent in the dispersion of the CNFs and (2) the benefit of the functionalization on the dispersion through the stability in the solvent and compatibility with

the matrix. The dispersion analysis of the materials leads to the conclusion that solvents containing oxygen groups work better with the oxidized CNFs, similarly solvents containing nitrogen groups with the nitrogen-functionalized CNFs. © 2012 Wiley Periodicals, Inc. *J Appl Polym Sci* 125: 3228–3238, 2012

**Key words:** carbon nanotube; composites; mechanical properties; dispersions; transmission electron microscope

## INTRODUCTION

Molecular  $sp^2$  filamentous-derived carbon architectures, that is, carbon nanotubes (CNTs) and carbon nanofibers (CNFs), have been widely investigated because of its exceptional properties<sup>1–3</sup> and the possibility of being incorporated into different matrices, such as polymers, resulting into novel functional materials.

One of the biggest challenges on developing high performance composite materials is obtaining a uniform dispersion of the filaments in the matrix. Unfortunately, CNTs and CNFs tend to form bundles (due to their high dispersive surface) and nests (due to the production method), making composite manufacturing difficult and tough. Several methods have been presented to disaggregate them from filament treatments<sup>4,5</sup> to composite fabrication.<sup>4–6</sup> Functionalization treatments may contribute to the separation of the filament nests, and, moreover, the chemical surface groups make the filaments more compatible with the polymer, favoring a stronger interface. Regarding the fabrication of the materials, the techniques that reduce the viscosity of the polymer, especially in thermoplastic matrices, use to achieve better results.<sup>4</sup> Similarly, solution methods became a good alternative.

Several reports show the improvement on the polymer properties by adding pristine and functionalized

CNTs in solvent processing performed in different solvents. Ramanathan et al.<sup>7</sup> reinforced a poly(methyl methacrylate) (PMMA) matrix with amino-functionalized singlewall carbon nanotubes (SWCNTs) by solvent mixing with *N,N*-dimethylformamide (DMF); Mathur et al.<sup>8</sup> enhanced electrical and mechanical properties of PMMA with carboxy-functionalized multiwall carbon nanotubes (MWCNTs) by solvent casting using toluene; Liu et al.<sup>9</sup> used nitromethane to fabricate CNT/PMMA and CNF/PMMA composites, achieving better electrical and mechanical properties than raw PMMA and so a large number of works can be mentioned.<sup>10–13</sup>

Liu et al.<sup>14</sup> highlighted the role of the solvent in the dispersion of pristine SWCNTs in solvent processed PMMA composites, concluding that the most homogeneous dispersion was achieved when the polar solubility parameter component ( $\delta_p$ ) of the solvent was higher than the corresponding  $\delta_p$  value of the PMMA. In this article, we study the effect of the solvent in the dispersion of CNFs in PMMA composites, but also the importance of the functional groups on treated CNFs to improve the affinity with the solvent and the compatibility with the matrix, and, in addition, the final dispersion. For these purposes, solvent processing was repeated in eight different solvents (acetone, *N*-methyl pyrrolidone, ethyl acetate, *N,N*-dimethylacetamide [DMAc], DMF, methyl ethyl ketone [MEK], tetrahydrofuran [THF], and toluene), in which the PMMA was soluble, and pristine, carboxylated, and amino-functionalized CNFs were used. Besides dispersion, mechanical properties of the composites were also evaluated.

Correspondence to: I. Martin-Gullon (gullon@ua.es).

## EXPERIMENTAL SECTION

### Materials

A commercial grade of PMMA Altuglas was used. Commercial helical-ribbon CNFs and Grupo Antolin CNFs were supplied by Grupo Antolin Ingenieria (Burgos, Spain). Characterization of these CNFs can be found elsewhere.<sup>15–17</sup> Solvents: acetone, *N*-methyl pyrrolidine (NMP), ethyl acetate, DMAc, DMF, MEK, THF, and toluene as well as acid nitric, ethylenediamine, and the coupling agent *N*-[(dimethylamino)-1*H*-1,2,3-triazolo[4,5,6]pyridin-1-ylmethylene]-*N*-methylmethanaminium hexafluorophosphate *N*-oxide (HATU) were purchased from by Sigma-Aldrich (Madrid, Spain) and VWR (Barcelona, Spain).

### Functionalization of CNFs

Carboxy-functionalized CNFs (O-CNF) were prepared from CNFs, as received, by oxidation with concentrated nitric acid (65 vol %) at 65°C for 12 h. Amine functionalization (N-CNF) consists of a direct coupling of ethylenediamine, performed by the coupling agent HATU,<sup>7</sup> on the carboxylic groups, previously introduced in the treatment with nitric acid.

We also include the demineralized CNFs (CNF-HCl) within the results. The demineralization treatment removes the mineral matter from remaining catalyst, without modifying the surface chemistry or the structure of the nanofilaments. It basically consists of a diluted HCl washing at room temperature for 12 h, followed of water washings to remove the acid. It has been observed that mineral matter can distort the characterization results in the pristine CNFs, so the demineralized CNFs can be a better blank to compare the effectiveness of the functionalization.

Functionalized CNF were characterized by X-ray spectroscopy (XPS), acid–base titration, and Fourier transform infrared spectroscopy (FTIR). XPS was carried out in a VG-Microtech Multilab 3000 equipment. Acid–base titration was used to determine acid, carboxylic, and basic surface groups.<sup>18</sup> For acid groups, samples were digested in NaOH for 24 h, and the filtrate was back-titrated with HCl; for basic groups, samples were digested with HCl, and the filtrate was back-titrated with NaOH; finally, carboxylic groups could be calculated by digestion with NaHCO<sub>3</sub> and titration of the filtrate with HCl. FTIR was performed in a BRUKER IFS 66 spectrometer.

### Composite preparation

CNFs were dispersed in the particular solvent by high shear rotor stator stirrer (Silverson LR4T, Silverson Machines, MA) at 8000 rpm for 10 min to form a suspension of 1 wt % CNFs. An appropriate amount of PMMA for 1 wt % CNF composites was

dissolved in the minimum amount of solvent in another container. The dispersed CNFs suspension and the dissolved PMMA were combined and mixed first via magnetic stirring for 30 min and then via high shear mixing for 10 extra min. The final mix was spread in a tray and dried for 24 h in the vacuum oven. Nanocomposites at 1 wt % of pristine (used as received), carboxylated, and amino-functionalized CNFs were prepared, for each solvent, to have a total of 24 different composites.

Specimens for mechanical properties and dispersion analysis were prepared in a laboratory hot plate press (Carver) at 150°C for 10 min at 2 ton. Dog-bone and rectangular specimens for tensile and flexural tests, respectively, were prepared regarding specifications of UNE EN ISO 527<sup>19</sup> for tensile specimens and ASTM D 790<sup>20</sup> for flexural specimens using an aluminum mold. The rough surfaces of the specimens were smoothed by polishing.

### Dispersion

Dispersion was evaluated by two different methods. First, the level of dispersion at micron scale (microdispersion) was evaluated by confocal microscopy at 40× magnification in a LEICA confocal microscope, using a laser of Argon. The hot-pressed samples were cut using a microtome, into slices of 10 μm thick with a glass blade. Samples processed by solvent provide confocal microscopy images where textures, instead of real agglomerations, can be observed, depending on the homogeneity of the dispersion and the affinity polymer-filler. In this case, the quality of the dispersion is evaluated by the MATLAB “imhist” command that examines and plots 256 tonalities of the grey scale, which are related with the uniformity of the dispersion, generating a histogram where the x-label corresponds to the grey scale and the y-label to the number of pixels of the image that are in a specific value of the grey scale.

In the second method, transmission electron microscopy ultramicrotomy was used to examine dispersion on the nanoscale. The composite samples were cut with a diamond blade yielding thin slices between 80 and 120 nm thick. A total area of 750 μm<sup>2</sup> was examined, which is an area 2000 times smaller than the explored with confocal microscopy. The electron transparent slices were imaged in a JEOL 2010 transmission electron microscope (TEM).

### Mechanical properties

The tensile and flexural properties of the composites were determined using the standard set forth in UNE EN ISO 527<sup>19</sup> and ASTM D 790,<sup>20</sup> respectively. The cross-head rates were 0.5 mm min<sup>-1</sup> for tensile

tests and  $1.37 \text{ mm min}^{-1}$  for flexural tests. The tests were performed on an INSTRON dynamometer, model 3344.

## RESULTS AND DISCUSSION

### Functionalization

The surface composition of carbon, oxygen, and nitrogen determined by XPS of the pristine and functionalized CNFs is shown in Table I. The oxygen content is quite high in the pristine filaments, but decreases in the HCl washed sample, confirming the distortion of the XPS results by the remaining catalyst. Comparing with the demineralized CNFs, the amount of oxygen is increased in the acid treatment. The reaction with ethylenediamine produces a decrease in the oxygen wt %, as expected by the replacement of the carboxylic groups by amine groups.<sup>21</sup> The XPS detects nitrogen just in the sample treated with the ethylenediamine.

Concentration on total acid groups, carboxylic groups, and basic groups is included in Table II. Noted again is the decrease in the content of oxygen groups and basic groups, when demineralizing the pristine sample, and the small amount of carboxylic groups in the unmodified CNFs. The concentration of carboxylic groups increases with the nitric acid treatment, while becomes zero after reaction with ethylenediamine. This means that all carboxylic groups have been replaced by nitrogen groups, which confers basic character of the CNF surface.<sup>22</sup>

Figure 1 shows the spectra of the treated and untreated CNFs in the span between 1000 and 1900  $\text{cm}^{-1}$ , where significant changes were found. The C=O stretch appears in the spectrum of the carboxylated CNFs approximately  $1749 \text{ cm}^{-1}$ .<sup>21</sup> This peak disappears in the spectrum of the nitrogen-functionalized CNFs and a new one arises at  $1683 \text{ cm}^{-1}$ , which is attributed to the amide carbonyl (C=O—NH—) stretch<sup>21</sup> introduced in the direct coupling of the ethylenediamine.

### Dispersion

In solvent processing, compatibility between the solvent and the filaments seems to be a key factor to achieve good dispersion. Liu et al.<sup>14</sup> studied the dis-

**TABLE I**  
Weight Concentration in Carbon, Oxygen, and Nitrogen by XPS

Sample	C (%)	O (%)	N (%)
CNF	89.00	11.00	0
CNFs-HCl	91.74	8.26	0
O-CNF	88.16	11.84	0
N-CNF	86.60	10.22	3.17

**TABLE II**  
Concentration on Acid, Carboxylic, and Basic Groups Determined by Acid-Base Titration

Sample	Total acid groups ( $\text{mmol g}^{-1}$ )	Carboxylic groups ( $\text{mmol g}^{-1}$ )	Total basic groups ( $\text{mmol g}^{-1}$ )
CNF	0.904	0.022	2.180
CNF-HCl	0.487	—	0.194
O-CNF	0.883	0.237	0
N-CNF	0.839	0	0.690

persion of unmodified SWCNTs in PMMA in several solvents varying solubility parameters. They concluded that the most homogeneous dispersion was achieved when the polar solubility parameter component ( $\delta_p$ ) of the solvent was higher than the corresponding  $\delta_p$  value of the PMMA. According to this statement, dispersion of the composites should be very poor in toluene, regular in ethyl acetate and THF, should improve in MEK and acetone, and should be even better in DMAc, NMP, and DMF. On the other hand, dispersion in the same solvent can be modified with the functionalities introduced in the treated CNFs.

An example of the different achieved dispersion, depending on the solvent and the type of CNFs (treated or untreated), is shown in the confocal microscopy and TEM micrographs of the composites processed in toluene (Fig. 2), acetone (Fig. 3), ethyl acetate (Fig. 4), DMF (Fig. 5), and NMP (Fig. 6). Confocal microscopic micrographs come with representative histograms of the distribution of the image pixels in the grey scale.

The dispersion in toluene at the microscale is quite poor in all cases (Fig. 2). It is acceptable with CNF, seems to be less homogeneous with O-CNF, and lightly better with N-CNF, although some nests can be still seen. The histograms of the samples containing CNF and O-CNF are asymmetric, while the

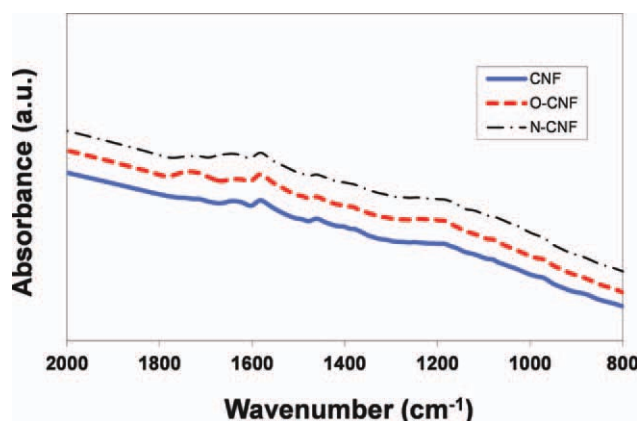


**Figure 1** FTIR spectra of the pristine and treated CNFs. [Color figure can be viewed in the online issue, which is available at [wileyonlinelibrary.com](http://wileyonlinelibrary.com).]



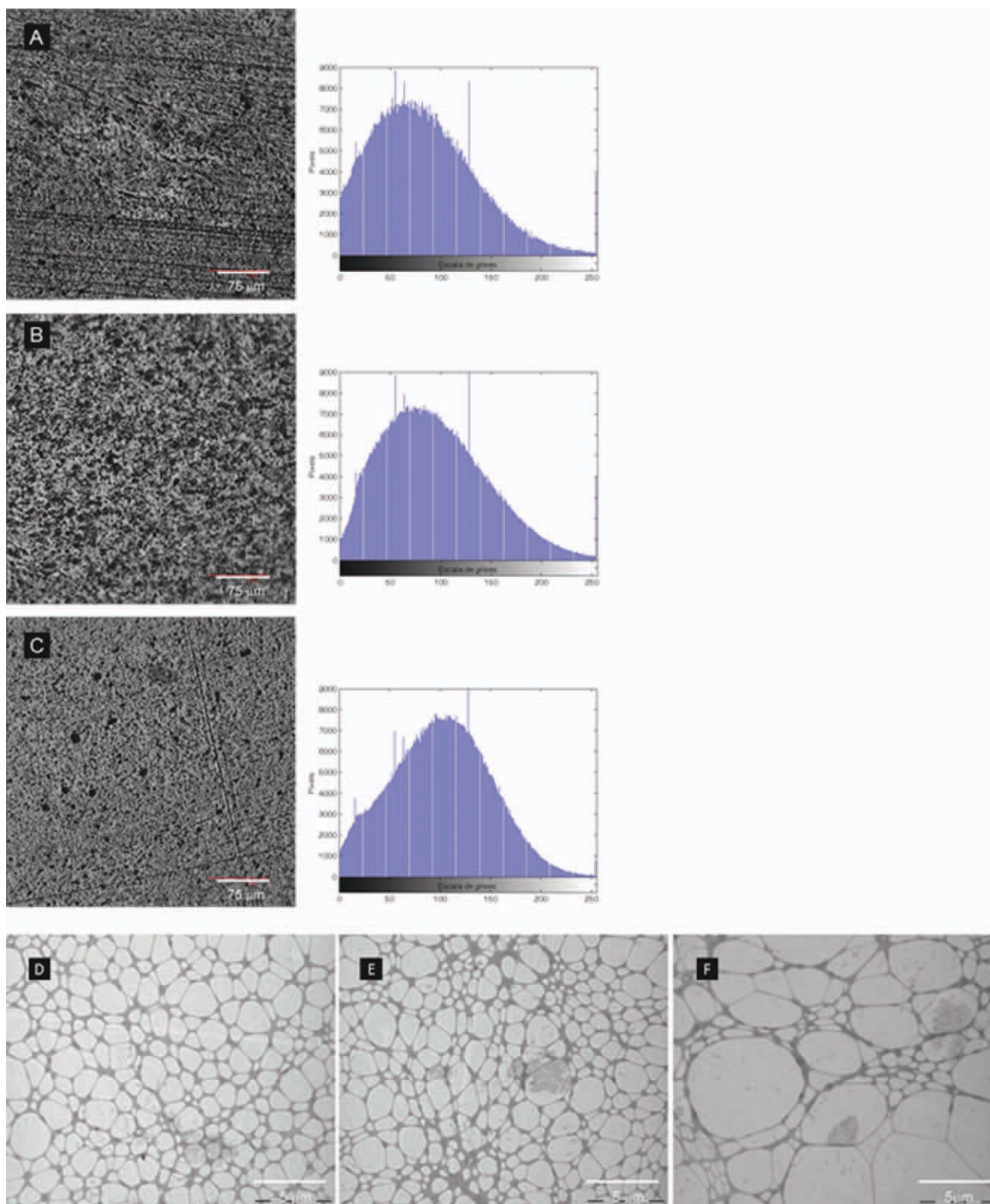


**Figure 2** Composites processed in toluene. Confocal microscopy micrographs: CNFs (A), O-CNFs (B), and N-CNFs (C) and TEM micrographs: CNFs (D), O-CNFs (E), and N-CNFs (F). [Color figure can be viewed in the online issue, which is available at [wileyonlinelibrary.com](http://wileyonlinelibrary.com).]

histogram of the sample with N-CNF is more symmetric, indicating more homogeneity in the further case. In the TEM micrographs (Fig. 2), clear zones

without fibers appear with clusters of approximately 2 μm size. Some individual N-CNF can also be observed [Fig. 2(F)].

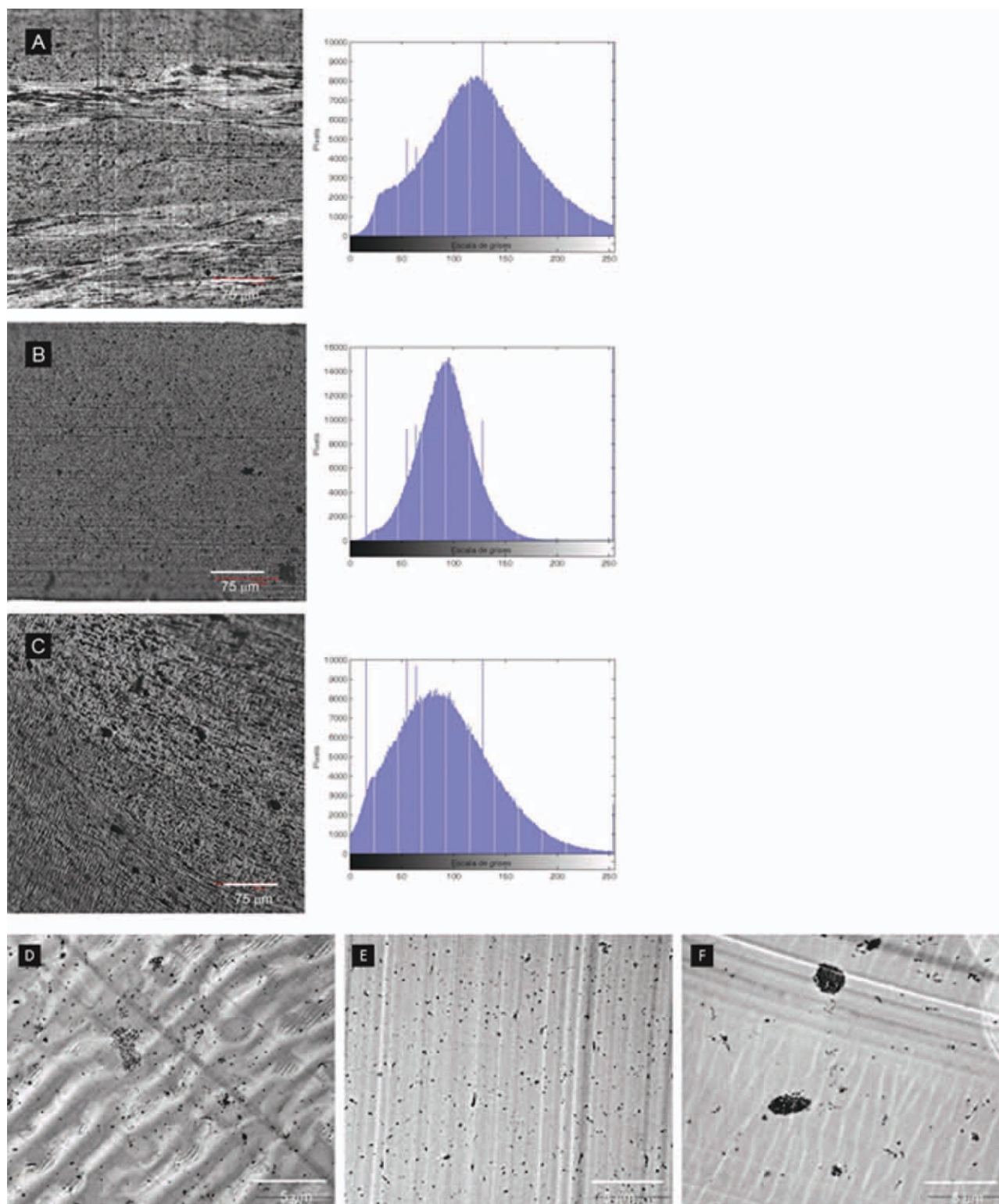


**Figure 3** Composites processed in acetone. Confocal microscopy micrographs: CNFs (A), O-CNFs (B), and N-CNFs (C) and TEM micrographs: CNFs (D), O-CNFs (E), and N-CNFs (F). [Color figure can be viewed in the online issue, which is available at [wileyonlinelibrary.com](http://wileyonlinelibrary.com).]

The dispersion and trend shown by acetone (Fig. 3) and ethyl acetate (Fig. 4) are similar: segregation of pristine CNFs, but homogeneity of functionalized CNFs. In acetone, and in ethyl acetate,

the dispersion of O-CNF is nearly perfect [Figs. 3(B) and 4(B)], achieving individual dispersion of the filaments [Figs. 3(E) and 4(E)]. The histogram of the material with the untreated CNFs has



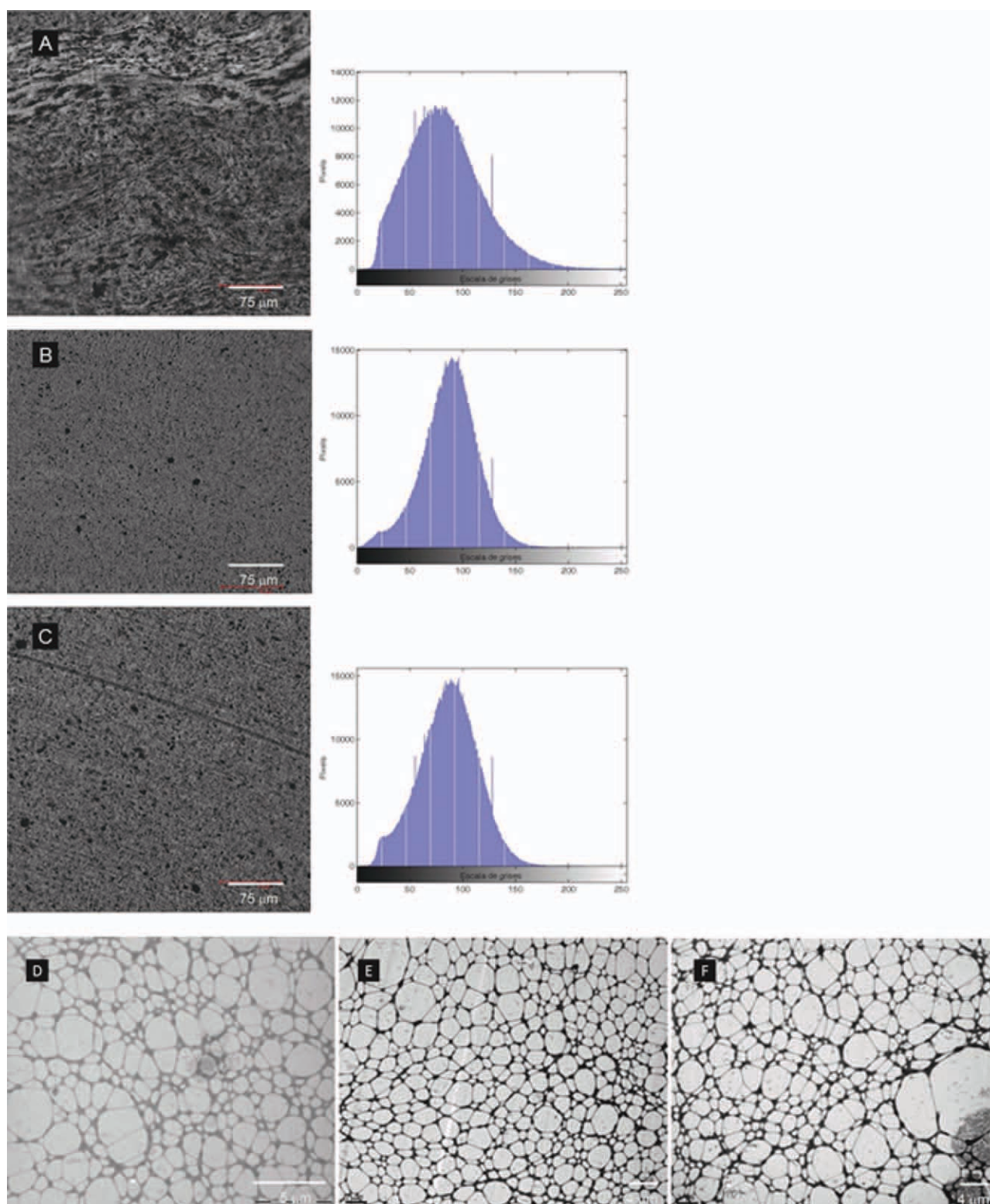


**Figure 4** Composites processed in ethyl acetate. Confocal microscopy micrographs: CNFs (A), O-CNFs (B), and N-CNFs (C) and TEM micrographs: CNFs (D), O-CNFs (E), and N-CNFs (F). [Color figure can be viewed in the online issue, which is available at [wileyonlinelibrary.com](http://wileyonlinelibrary.com).]

Gaussian shape, almost symmetric, disrupted by the presence of some nests, and wide, due to the difference on intensities created by the segregation of phases (the CNF suspension into the dissolved

PMMA). The histogram of the material with O-CNF is a narrow symmetric peak [Fig. 3(B) and 4(B)], which is a characteristic of homogeneous dispersions.

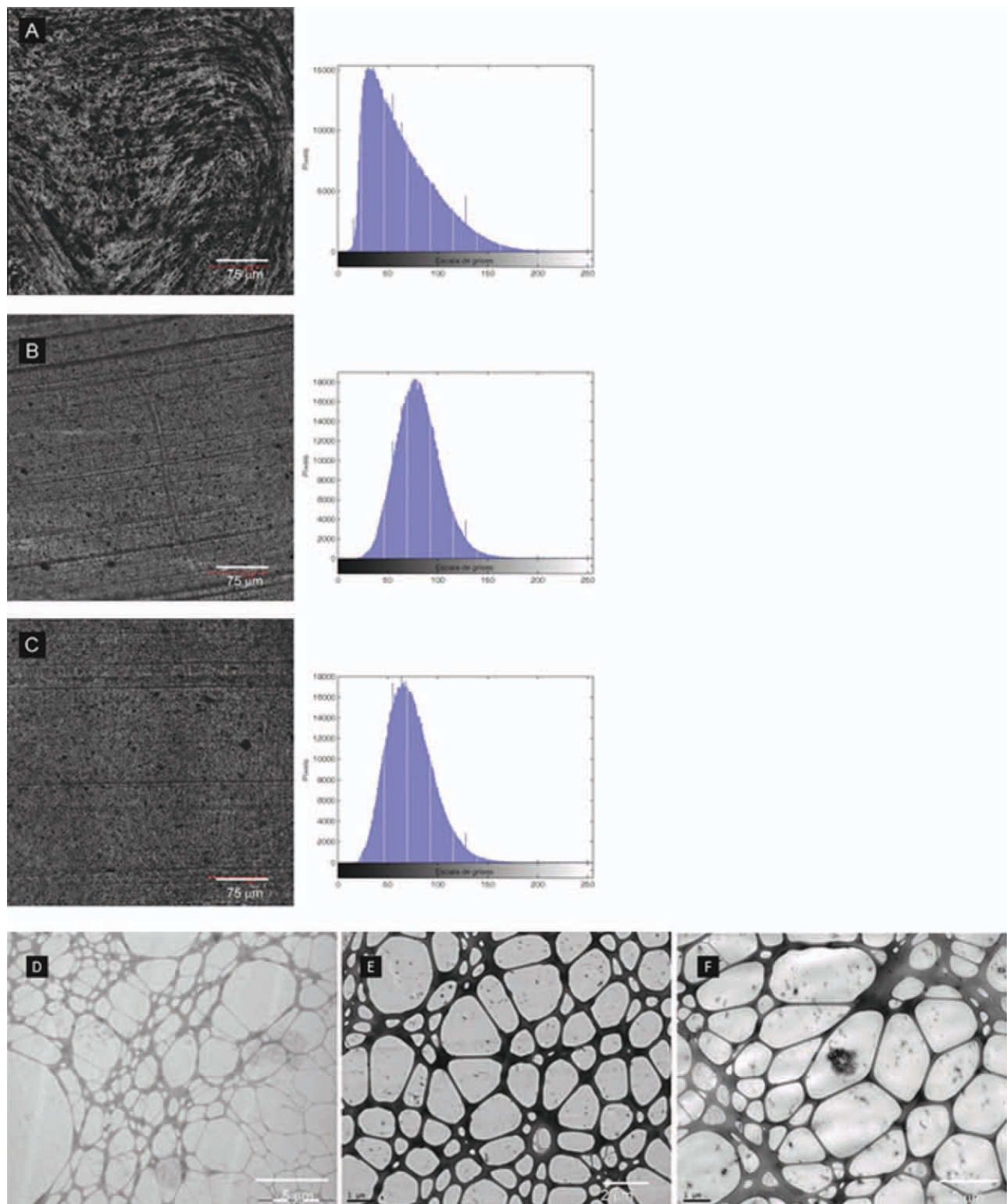


**Figure 5** Composites processed in DMF. Confocal microscopy micrographs: CNFs (A), O-CNFs (B), and N-CNFs (C) and TEM micrographs: CNFs (D), O-CNFs (E), and N-CNFs (F). [Color figure can be viewed in the online issue, which is available at [wileyonlinelibrary.com](http://wileyonlinelibrary.com).]

Dispersion of unmodified CNFs in the composites processed in DMF (Fig. 5), NMP (Fig. 6), and DMAc (not shown because the trend is the same as in DMF and NMP) is poorer than in acetone and ethyl ace-

tate, but it is improved in the nanocomposites containing the functionalized CNFs, as can also be observed in the more symmetric and narrower histograms (Figs. 5 and 6). The same trend is noticed at



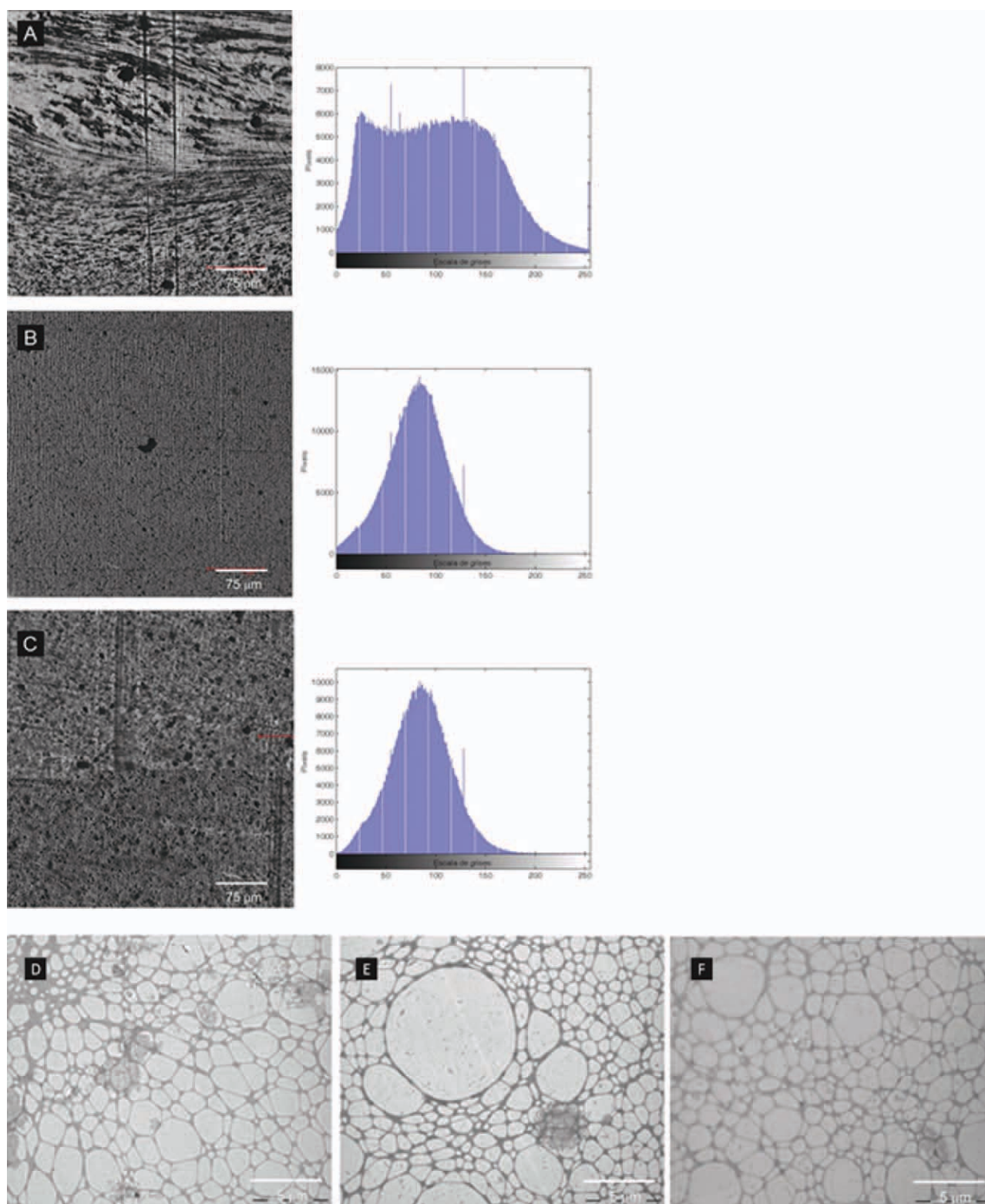


**Figure 6** Composites processed in NMP. Confocal microscopy micrographs: CNFs (A), O-CNFs (B), and N-CNFs (C) and TEM micrographs: CNFs (D), O-CNFs (E), and N-CNFs (F). [Color figure can be viewed in the online issue, which is available at [wileyonlinelibrary.com](http://wileyonlinelibrary.com).]

the TEM micrographs with better distribution of O-CNF and N-CNF, which are even isolated (Fig. 5 and 6).

Functionalization dramatically improves dispersion in solvent processing by favoring affinity with the solvent and compatibility with the matrix.



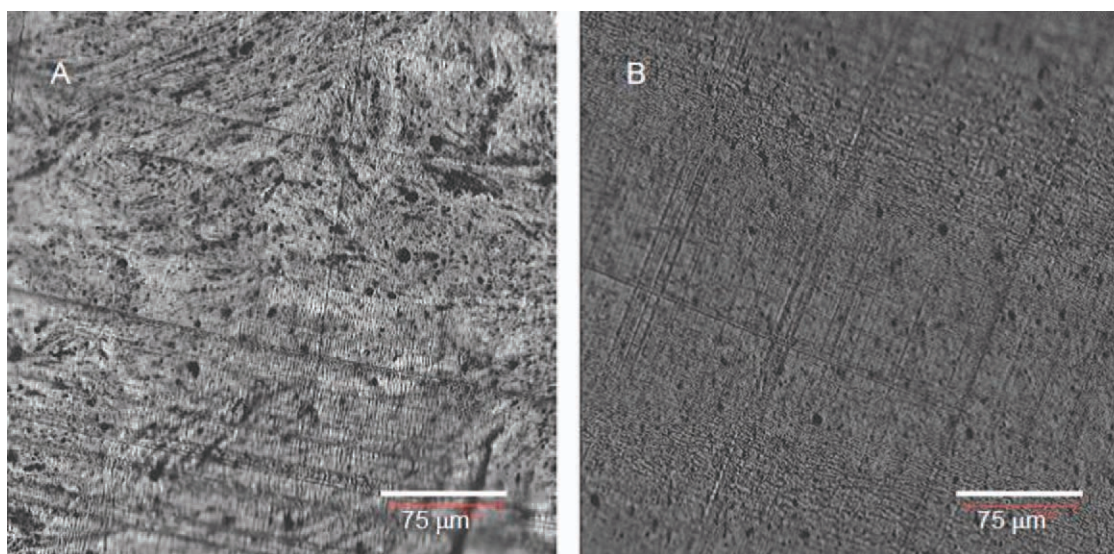


**Figure 7** Composites processed in acetone with (A) CNFs and (B) O-CNFs after various hot plate pressings. [Color figure can be viewed in the online issue, which is available at [wileyonlinelibrary.com](http://wileyonlinelibrary.com).]

Moreover, it can be noticed that solvents containing oxygen groups as acetone and ethyl acetate present more affinity for O-CNF, similarly solvents with nitrogen groups for N-CNF, except for NMP.

It is important to take into account that in the casting processing, the solvent is freely evaporated. The pristine CNF/PMMA films prepared in the more volatile solvents, as acetone or ethyl acetate, have better appearance than those processed in DMF or NMP, with slow evaporation rates. However, when the functionalized CNFs are used, the evaporation rate of the solvent does not seem to be so important, as observed in the images. Meanwhile, the material is in a fluid state, the fibers can move and will keep dispersed once the solvent is evaporated. Slow evaporation rate of the solvent, poor affinity between the solvent and the fibers, and poor compatibility between the fibers and the matrix can favor the reagglomeration, when they can still move. If the evaporation rate is high, the particles are quickly held by the polymer, keeping the achieved dispersion during mixing. As the functionalization improves the affinity and compatibility with the solvent and the matrix, reagglomeration is less favored, even with solvents that slowly evaporate. Besides the difference of polarity between the solvent and the polymer, as proposed by Lui et al.,<sup>14</sup> it is also important the affinity between the solvent and the CNFs that will provide a more stable suspension and, consequently, a better dispersion in the matrix. Moreover, the compatibility between the CNFs and the matrix can be improved, so the polymer can more efficiently intercalate the filaments, keeping them separated.

It is worth to notice that once the solvent is removed and the filaments are suitably dispersed,

the postprocessing does not require shear forces. The dispersion can be maintained during subsequent compression-moulding.<sup>4</sup> Figure 7 shows the confocal microscopy images of the composites processed in acetone with 1 wt % of CNF (A) and O-CNF (B) after several hot plate pressings. Comparing with Figure 3, the same composites pressed once, dispersion has not changed: it is still poor in the sample with pristine CNFs and better with O-CNF. The dispersion in the sample containing CNFs does not improve with the subsequent pressings; it seems that this is the best dispersion that can be achieved using this particular solvent process.

### Mechanical properties

The tensile properties (Strength, modulus, and elongation) of the samples processed in toluene, acetone, ethyl acetate, DMF, and NMP, containing the pristine and the functionalized CNFs, are shown in Figure 8.

In general, tensile properties slightly improve in toluene, acetone, and ethyl acetate. In acetone, modulus and strength increase in the samples containing functionalized CNFs with respect to the material containing the pristine CNFs, as expected, due to their better dispersion. Modulus is 5 and 6% higher with O-CNF and N-CNF, respectively, comparing with the 3% increase with CNF; strength rises to 16% with CNF and approximately 20% with O-CNF and N-CNF. In toluene, there is a small increase in modulus with CNF and O-CNF, but not with N-CNF, although this material seemed to be more homogeneous; strength is 27% higher in the sample with O-CNF comparing with the neat PMMA, followed by 19% increase with N-CNF and 17% with

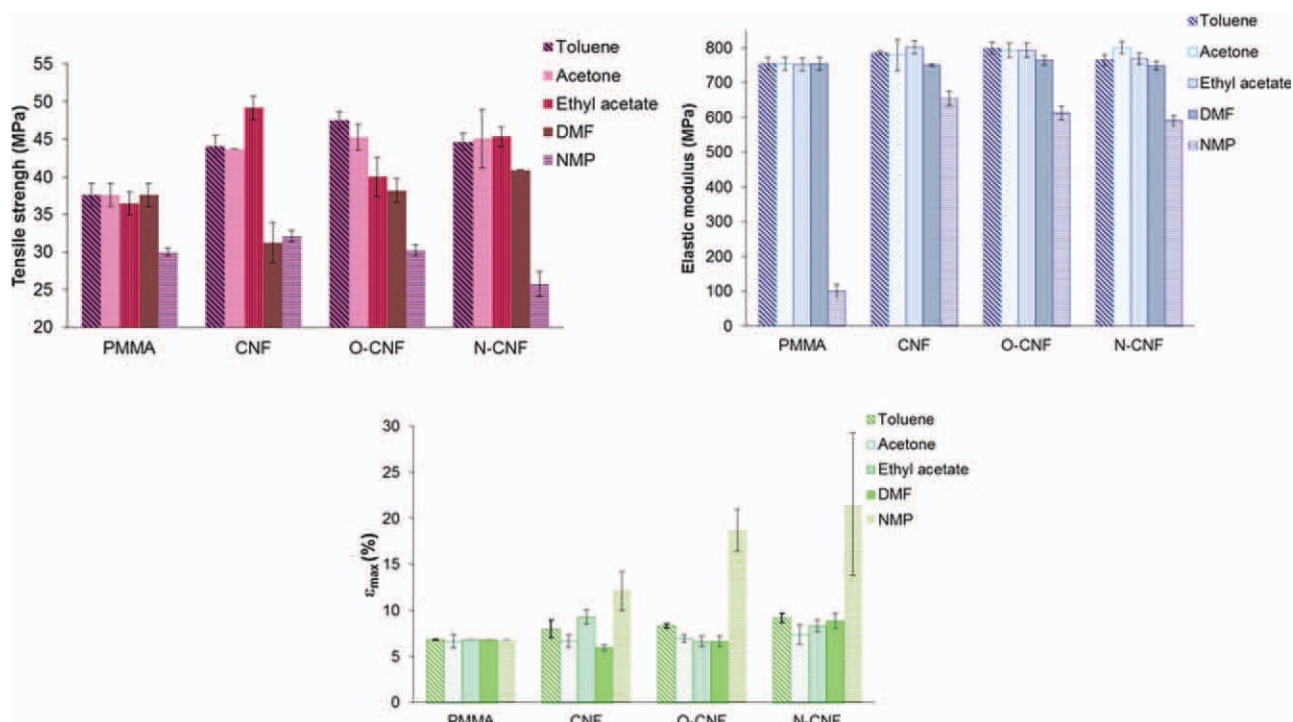


**Figure 8** Tensile (left) and flexural (right) properties of the solvent processed in acetone nanocomposites. [Color figure can be viewed in the online issue, which is available at [wileyonlinelibrary.com](http://wileyonlinelibrary.com).]

CNF. In ethyl acetate lightly better mechanical properties are achieved adding the unmodified CNFs than the functionalized CNFs. Increase in modulus is 6%, 5%, and 2% with CNF, O-CNF, and N-CNF, respectively, and, in the same order, 31%, 7%, and 21% in strength. In DMF, there is just an improvement in strength with N-CNF, in which dispersion was also quite homogeneous. Our mechanical experiments of the specimens processed in NMP are influenced by the presence of solvent and cannot be taken as a reference. We include the results just to show the effect of remaining solvent in the mechanical properties. Compared with the neat PMMA processed in NMP, the modulus dramatically increases when adding the CNFs, indicating a strong stiffening effect, besides the presence of solvent. On the other hand, compared with the other references of PMMA in which the effect of solvent was not observed, the modulus is clearly affected by its traces. The high increase in elongation is a clear indicative of the plastifying effect of the NMP in the composite material.<sup>8</sup>

It is interesting that the increase in elongation in toluene, acetone, ethyl acetate, and DMF (no effect of the solvent was observed), especially in those cases in which modulus increased, improves toughness. Normally, the addition of a filler to a polymer produces the stiffening and shortens elongation, but the opposite behavior has been observed here. It is believed, and some recent publications can

confirm it,<sup>23</sup> that the special structure of helical ribbon CNFs, consisting of a continuous spiral, can increase the polymer toughness by unraveling during the pull-out, if they are lightly bonded to the matrix.

Summarizing, it is quite difficult to extract certain conclusions about the mechanical properties of solvent processed composites, as can be affected by remaining solvent. In this particular case, the deterioration of the mechanical properties due to remaining solvent is just evident in the NMP samples. Anyway, the best results correspond to the materials fabricated with the lower boiling point solvents (acetone or ethyl acetate, for example) due to its faster and more efficient elimination. The same behavior was previously described by Lau et al.<sup>24</sup> in epoxy nanocomposites.

A wide enhancement range of the mechanical properties of PMMA by the addition of pristine and treated CNTs can be found in the literature.<sup>7,25,26</sup> Considering those results and the lower crystalline quality of CNFs compared with CNTs, the above results are satisfactory.

## CONCLUSION

In this article, we have evaluated and compared the effect of the solvent and the functionalization of CNFs in solvent processing of CNF/PMMA



nanocomposites. The importance of the particular solvent has been demonstrated as regards affinity with the filaments that will determine their dispersion in the matrix. CNF surface chemistry results clue to improve stability in the solvent and, therefore, homogeneous distribution in the polymer.

The mechanical properties were evaluated considering dispersion and possible interactions of the filaments with the matrix. In general, elastic modulus was enhanced with improved dispersion and functionalization. In addition, the better results correspond to the solvents that provide better dispersion and easily evaporate.

H.V.-R. thanks the Spanish Ministry of Education, FPU program.

## References

1. Lawrence, J. G.; Berhan, L. M.; Nadarajah, A. *ACS Nano* 2008, 2, 1230.
2. Tibbetts, G. G.; Lake, M. L.; Strong, K. L.; Rice, B. P. *Compos Sci Technol* 2007, 67, 1709.
3. Hammel, E.; Tang, X.; Trampert, M.; Schmitt, T.; Mauthner, K.; Eder, A.; Pötschke, P. *Carbon* 2004, 42, 1153.
4. Shaffer, M. S. P.; Sandler, J. K. W. In *Processing and Properties of Nanocomposites*; Advani, S., Ed.; World Scientific Publishing: Singapore, 2007; Chapter 1, p 1.
5. Advani, S. G. In *Processing and Properties of Nanocomposites*; Advani, S. G., Ed.; World Scientific Publishing: Singapore, 2007; Chapter 3, p 61.
6. Haggenueller, R.; Gommans, H. H.; Rinzler, A. G.; Fischer, J. E.; Winey, K. I. *Chem Phys Lett* 2000, 330, 219.
7. Ramanathan, T.; Liu, H.; Brinson, L. C. *J Polym Sci Pol Phys* 2004, 43, 2269.
8. Mathur, R. B.; Shailaja, P.; Singh, B. P.; Dhama, T. L. *Polym Compos* 2008, 29, 717.
9. Liu, J.; Rasheed, A.; Minus, M. L.; Kumar, S. *J Appl Polym Sci* 2009, 112, 142.
10. Zhang, K.; Lim, J. Y.; Choi, H. J. *Diam Relat Mater* 2009, 18, 316.
11. Valentini, L.; Bittolo-Bon, S.; Kenny, J. M. *Macromol Mater Eng* 2008, 293, 867.
12. Dai, J.; Wang, Q.; Li, W.; Wei, Z.; Xu, G. *Mater Lett* 2007, 61, 27.
13. Du, F.; Fischer, J. E.; Winey, K. I. *J Polym Sci Pol Phys* 2003, 41, 3333.
14. Liu, J.; Liu, T.; Kumar, S. *Polymer* 2005, 46, 3419.
15. Martin-Gullon, I.; Vera, J.; Conesa, J. A.; Gonzalez, J. L.; Merino, C. *Carbon* 2006, 44, 1572.
16. Vera-Agullo, J.; Varela-Rizo, H.; Conesa, J. A.; Almansa, C.; Merino, C.; Martin-Gullon, I. *Carbon* 2007, 45, 2751.
17. Vera-Agullo, J.; Varela-Rizo, H.; Font, R.; Conesa, J. A.; Martin-Gullon, I. *J. Anal Appl Pyrolysis* 2007, 79, 484.
18. Boehm, H. P. *Adv Catal* 1966, 16, 179.
19. UNE-EN-ISO 527-1: Determinación de las propiedades de tracción. Parte 1: Principios generales. AENOR, Madrid, España, 1996.
20. ASTM D 790: Standard test methods for flexural properties of unreinforced and reinforced plastics and electrical insulating materials. ASTM international, West Conshohocken, PA, United States, 1999.
21. Ramanathan, T.; Fisher, F. T.; Ruoff, R. S.; Brinson, L. C. *Chem Mater* 2005, 17, 1290.
22. Boehm, H. P. *Carbon* 1994, 32, 759.
23. Palmeri, M. J.; Putz, K. W.; Brinson, L. C. *ACS Nano* 2010, 4, 425.
24. Lau, K.-T.; Lu, M.; Chun-ki, L.; Cheung, H.-Y.; Sheng, F.-L.; Li, H.-L. *Compos Sci Technol* 2005, 65, 719.
25. Pande, S.; Mathur, R. B.; Singh, B. P.; Dhama, T. L. *Polym Compos* 2009, 30, 1312.
26. Velasco-Santos, C.; Martinez-Hernandez, A. L.; Fisher, F. T.; Ruoff, R.; Castaño, V. M. *Chem Mater* 2003, 15, 4470.